NIH Public Access
Author Manuscript
J Immunol. Author manuscript; available in PMC 2014 June 01.

Published in final edited form as:
J Immunol. 2013 June 1; 190(11): . doi:10.4049/jimmunol.1203548.

Rational engineering of a minimized immune inhibitor with unique triple targeting properties

Christoph Q. Schmidt[*,†], **Hongjun Bai**[*], **Zhuoer Lin**[*], **Antonio M. Risitano**[§], **Paul N. Barlow**[¶], **Daniel Ricklin**[*,1], and **John D. Lambris**[*,1]

[*]Department of Pathology & Laboratory Medicine, University of Pennsylvania, Philadelphia, USA

[†]Institute of Pharmacology of Natural Products and Clinical Pharmacology, Ulm University, Ulm, Germany

[§]Hematology, Department of Biochemistry and Medical Biotechnologies, Federico II University, Naples, Italy

[¶]Schools of Chemistry and Biological Sciences, University of Edinburgh, Edinburgh EH9 3JJ, United Kingdom

Abstract

Inadequate control of the complement system is the underlying or aggravating factor in many human diseases. While treatment options that specifically target the alternative pathway (AP) of complement activation are considered highly desirable, no such option is available in the clinic. Here we present a successful example of protein engineering, guided by structural insight on the complement regulator factor H (FH), yielding a novel complement-targeted therapeutic (mini-FH) with clinical potential. Despite a 70% reduction in size, mini-FH retained and in some respects exceeded the regulatory activity and cell surface-recognition properties of its parent protein FH, including the recently described recognition of sites of oxidative stress. Importantly, the chosen design extended the functional spectrum of the inhibitor, as mini-FH showed increased binding to the surface-bound opsonins iC3b and C3dg when compared to FH. Thus, mini-FH is equipped with a unique and clinically valuable triple-targeting profile towards diseased host cells, through its binding to sites of ongoing complement activation, markers of oxidative damage, and host surface-specific polyanions. When assessed in a clinically relevant AP-mediated disease model of paroxysmal nocturnal hemoglobinuria, mini-FH largely outperformed factor H and indicated advantages over clinically evaluated AP inhibitors. Thus, the rational engineering of a streamlined FH construct not only provided insight into the function of a key complement regulator but also yielded a novel inhibitor that combines a triple targeting approach with high AP-specific inhibitory activity (IC_{50} ~ 40 nM), which may pave the way towards new options for the treatment of complement-mediated diseases.

Introduction

Complement is integral to the immune system and contributes to host defense, immunomodulation and tissue homeostasis (1). The sensing of danger-associated molecular patterns on immune complexes, apoptotic cells or invading microorganisms triggers the

Address correspondence to: John D. Lambris, Department of Pathology & Laboratory Medicine, University of Pennsylvania, Philadelphia, Pennsylvania, USA. Fax: 215-573-8738, Phone: 215-746-5765, lambris@upenn.edu.
[1]D.R. and J.D.L. shared supervision of this study.

Competing financial interests: CQS, DR and JDL are inventors of a patent application that describes the use of mini-FH for therapeutic applications. JDL is the founder of Amyndas Biopharmaceuticals, which develops complement therapeutics.

NIH-PA Author Manuscript
NIH-PA Author Manuscript
NIH-PA Author Manuscript

NIH-PA Author Manuscript

NIH-PA Author Manuscript

NIH-PA Author Manuscript

activation of complement (2). Fixation of the opsonin C3b facilitates clearance by the reticulo-endothelial system and initiates a proteolytic cascade that generates potent effector molecules, which either recruit and activate immune cells or induce complement-mediated lysis of susceptible cells. Crucially, cell-surface-bound C3b also induces self-amplification via the alternative pathway (AP), in which it forms C3 convertases that cleave C3 and deposit additional C3b on target surfaces. While unrestricted amplification contributes to rapid elimination or destruction of opsonized particles, healthy host cells are usually protected by a panel of membrane-bound and soluble regulators (3), which destabilize the C3 convertase (decay acceleration activity), mediate the degradation of C3b to its cleavage products iC3b and C3dg that cannot form convertases but participate in signaling events (cofactor activity) or prevent the formation of lytic pores. Complement thereby critically relies on this concerted interplay between pattern recognition, activation and regulation mechanisms to provide a triage system that protects host tissue, clears cellular debris and induces forceful immune responses to eliminate microbial intruders.

Conversely, inadequately triggered, prolonged or insufficiently controlled complement activation is causative for, or associated with, several immune, inflammatory, age-related, and hemolytic disorders. In paroxysmal nocturnal hemoglobinuria (PNH), for example, the lack of some surface-bound regulators on blood cells leads to perpetual local activation of complement that causes erythrocyte lysis and platelet activation with severe clinical consequences, including high risk of thrombosis (4). The involvement of complement in the pathology of prevalent diseases such as age-related macular degeneration (AMD), together with its upstream role in controlling inflammatory processes, has fueled efforts to design complement-targeted therapeutics. However, several challenges have limited the development of efficient and cost-effective options (5). These include a lack of the detailed knowledge needed to guide design and engineering, the high plasma concentrations of some complement proteins, and finally, concerns that long-term systemic complement inhibition might interfere with complement's defensive functions, even though clinically evaluated complement inhibitors generally showed beneficial safety profiles (6). Currently available complement therapeutics either block a single initiation pathway (*i.e.*, C1 inhibitor; C1-INH) or inhibit the generation of specific effector molecules (*i.e.*, the C5-antibody Eculizumab). However, neither drug inhibits amplification of the complement response via the AP, which often contributes a majority of the overall complement response (5, 7). In the case of PNH, Eculizumab effectively prevents intravascular lysis of erythrocytes but does not alleviate perpetual opsonization that may cause extravascular lysis, thereby leaving about one third of patients still requiring erythrocyte transfusions (8, 9). In addition, both drugs primarily act in circulation rather than on diseased or damaged surfaces that are most likely to trigger complement-mediated inflammation; finally, C1-INH and Eculizumab are highly expensive in clinical use. An inhibitory option that preferentially controls AP amplification on target surfaces would therefore be desired as it holds the promise of requiring lower inhibitor doses while interfering less with immune surveillance functions of complement (10-12).

The soluble regulator factor H (FH), with its AP-directed activity and ability to recognize self-structures, represents a particularly promising candidate for therapeutically restoring the balance between complement activation and regulation on diseased cells. Concurrent recognition of C3b opsonins and polyanionic host-surface markers such as glycosaminoglycans (GAGs) enable FH to control complement activation effectively on self but not on foreign surfaces (13, 14) (Fig. 1A). In addition, FH has recently been identified as a recognition molecule for cellular pattern of oxidative stress such as malondialdehyde (MDA), with potential implications for AMD and other diseases (15). While the regulatory functions of FH are confined in the four N-terminal complement control protein (CCP) domains of this elongated and probably flexible plasma glycoprotein (16), self-cell specificity depends mainly on the simultaneous binding of the C-terminus (FH CCP19-20)

NIH-PA Author Manuscript

NIH-PA Author Manuscript

NIH-PA Author Manuscript

to polyanionic markers and C3b (17-19). Even though all opsonic fragments of C3 share a common binding site for CCP19-20 of FH (*i.e.,* the thioester-containing domain; TED), intact FH binds only very inefficiently, or not at all, to the proteolytically processed degradation products of C3b (*i.e.,* iC3b), which accumulate on the target surface and thereby represent hallmarks of ongoing complement activation under disease conditions (20, 21). Because the recombinant bimodule FH19-20 strongly binds to both iC3b and C3dg (14), it seems probable that the middle region of FH (CCP5-18) masks the C-terminal recognition domains within full-length FH from engaging C3b-inactivation products under physiological conditions (22). Therefore, modifications of the 155-kDa glycoprotein FH, which do not tamper with the regulatory functions but reduce its size and complexity (*e.g.,* by omitting N-glycosylation) and reveal cryptic sites needed for binding to sites of high opsonic turnover, represent an attractive path toward specific and potent complement inhibitors. The benefit of targeting the regulatory functions of FH to diseased surfaces, which are characterized by ongoing complement activation, has been proven by the biopharmaceutical drug TT30 (Alexion Pharmaceuticals) (23). TT30 utilizes four CCP domains of complement receptor 2 (CR2; CD21) as an N-terminal iC3b/C3dg-targeting moiety, which is fused to the first five CCP domains of FH that harbor the complement regulatory region (*i.e.*, FH CCP1-4) (23).

Based on the hypothesis of a cryptic recognition site within FH, and recent structural insight into the binding of FH1-4 to C3b and FH19-20 to C3dg (14, 24, 25), we developed a novel FH-based inhibitor (mini-FH) with expected advantages for therapeutic targeting. In contrast to TT30, our strategy solely relies on FH domains and unmasks the cryptic site of FH by rationally adapting its modular domain structure in order to facilitate targeting to C3-activation and inactivation products. In this way, by retaining all of FH's major C3b-binding domains at either terminus, our design warrants not only high affinity for C3b, iC3b and C3dg, but, importantly, also incorporates FH's recognition activity for host-specific polyanions and oxidative damage markers. Indeed, the resulting mini-FH features a unique triple targeting mechanism for simultaneous recognition of C3-activation/inactivation products, oxidative markers and host-surface markers, which substantially surpasses the template molecule FH in controlling AP-activation in complement-mediated disease conditions, as exemplified on PNH erythrocytes.

Material and Methods

Protein design and computational modeling

The structural model of the C3b:mini-FH complex was constructed by superimposing the TED/C3d domain of the C3b:FH1-4 (PDB accession no. 2WII) (24) and C3d:FH19-20 (PDB 3OXU) (14) complex structures. The root mean square distance between two superposed C3d domains was 0.285 Å. The linker between CCP4 and CCP19, containing between 9 and 18 consecutive glycine residues, was modeled by the dope_loopmodel module of MODELLER 9v8 (26). The energy of dope_loopmodel, which provides the energyscore that we used to evaluate the models of mini-FH with different linker length when bound to C3b, is composed by several terms, including bond length, bond angle, torsion, improper torsion, dihedral, 6-12 Lennard-Jones potential, DOPE potential and GBSA solvent potential. For each linker length, 100 conformations were sampled. The top 80 models of each linker length were selected out to evaluate the effect of different length on energy and conformation.

Construction, expression and purification of mini-FH

A codon-optimized gene for mini-FH cloned into the *P. pastoris* expression vector pPICZαB (Invitrogen) was transformed into the expression strain KM71H (Invitrogen) and expressed in a fermenter in analogy to the recombinant control proteins FH1-4, FH19-20 and FH12-13,

NIH-PA Author Manuscript

NIH-PA Author Manuscript

NIH-PA Author Manuscript

which had been expressed and characterized as described before (13, 27). FH was initially precipitated from human plasma with 12% PEG-3350. All proteins were purified to homogeneity by applying successive ion exchange and size exclusion chromatography steps. The identity and purity of mini-FH were characterized using SDS-PAGE and mass spectrometry (Synapt G2; Waters).

Binding studies for C3-derived opsonins and markers of oxidative stress

Surface plasmon resonance (SPR) experiments were performed on a Biacore 3000 instrument (GE Healthcare), processed in Scrubber (v2.0c; BioLogic), and are shown as duplicates of reference surface-subtracted response curves. Equal amounts of C3b were immobilized onto three flow cells of a CM5 sensor chip (GE Healthcare) by convertase-mediated deposition by repetitive injections of a mix if factors B and D (500 nM and 200 nM, respectively) and C3 (1 μM) (28, 29). C3b molecules on two separate flow cells were processed with factor I (FI) in the presence of either FH or soluble complement receptor 1 (sCR1; Celldex Therapeutics) as cofactors to yield iC3b or C3dg, respectively. Successful processing to iC3b and C3dg was demonstrated with injections of FH15-18 (negative control) and sCR1, which showed strong binding to C3b, a weak response to iC3b and negligible binding to the C3dg surface, consistent with previous findings (21, 30). Deposition, proteolytic processing and all interaction studies were performed in HBS-P^+ buffer (10 mM HEPES pH 7.4, 150 mM NaCl, 0.005% Tween-20, 1 mM $MgCl_2$) at 25 °C. An ELISA-assay, based on previous studies (15), was employed to measure binding of FH-derived proteins to surfaces coated either with BSA modified with the lipid peroxidation product malondialdehyde-acetaldehyde (MAA-BSA) or with unmodified BSA. Bound analytes were detected with a polyclonal anti-FH Ab.

Functional characterization

The ability of different FH fragments and mini-FH to destabilize the AP C3 convertase (decay acceleration activity) was evaluated using SPR, as described before (31). Briefly, C3b molecules were immobilized onto a CM5 sensor chip (GE Healthcare) by convertase-mediated deposition as described above. A mix of 100 nM FD and 500 nM FB in running buffer (HBS-P+) was injected for 3 min at 10 μl/min over the C3b surface to build the convertase complex (C3bBb) on the chip. Following an undisturbed decay of 1 min, the analytes (either FH, FH1-4, FH19-20 or mini-FH; all at 100 nM) were injected for 3.5 min. To regenerate the surface, residual convertases were decayed by consecutive injections of 2 μM FH1-4 and 1M NaCl. For comparative visualization of the pure decay acceleration response, SPR binding signals of the analytes in the absence of the convertase were subtracted from the corresponding convertase decay response. Processed, superimposed sensorgrams were normalized to compensate for the small drift in signal due to the convertase-mediated immobilization procedure in order to facilitate an overlay of sensorgrams at the time point of analyte injection (the normalization was below 7% for all sensorgrams). Duplicate sensorgrams are shown to demonstrate reproducibility.

To assess the cofactor activity of FH and constructs thereof, a fluid phase, time-course cofactor assay was performed in PBS similar to previous descriptions (31). Briefly, solutions containing FI and C3b (0.01 μM and 0.7 μM, respectively; Complement Technology) and either FH or mini-FH as cofactor (0.1 μM; added last) were prepared on ice and aliquoted into 20-μl aliquots prior to incubation at 37 °C for increasing amount of time (5, 10, 20, 40 min). A mixture in absence of any cofactors served as negative control. Each reaction sample was analyzed by 9 % SDS-PAGE, stained using Coomassie, and evaluated for the cleavage of the α’ chain of C3b (113 kDa) into the smaller fragments (43, 46 and 68 kDa) present in iC3b.

NIH-PA Author Manuscript

NIH-PA Author Manuscript

NIH-PA Author Manuscript

Heparin chromatography

Glycosaminoglycan binding activity was evaluated as changes of retention time during heparin affinity chromatography. A 5 ml HiTrap heparin column (GE Healthcare) equilibrated in PBS pH 7.4 was used on a FPLC. After injecting a 1 ml-sample of each ligand resulting in an absorption of ~ 0.1 at 280 nm (*i.e.,* 63 μg FH, 57μg mini-FH, 62 μg FH1-4, 53 μg FH19-20), elution was performed by applying a linear gradient from PBS to PBS substituted with 0.5 M NaCl within 5 column volumes.

Inhibition of complement activation

Inhibition of complement activation via the classical or alternative pathway was determined by established ELISA-based assays (32) by coating plates with either ovalbumin antigen-antibody complexes (CP) or lipopolysaccharide (LPS) and adding diluted plasma in the presence of increasing concentrations of FH-based analytes. For assessing inhibition of the classical pathway by ELISA, 96-well plates (MaxiSorp; Nunc) were coated with 1% ovalbumin (Sigma; 50 μl/well) in PBS pH 7.4 for 2 h at room temperature (RT) or overnight at 4 °C. Washing twice with 200 μl/well PBST (PBS containing 0.05% Tween-20) was followed by blocking with 200 μl/well 1% BSA (bovine serum albumin) in PBS for 1 h at RT. Rabbit anti-ovalbumin antibody at a dilution of 1:1000 in 1% BSA/PBS was bound for 1 h at RT (50 μl/well). After another washing step, as above, serial dilutions of analytes in PBS were added to the 96 well plate. To 10 μl of analyte, 20 μl of PBS^{++} (PBS containing 1 mM $MgCl_2$ and 0.9 mM $CaCl_2$) was added into each well of the ELISA plate, followed by 30 μl of a 1:40 serum dilution in PBS^{++}. The mix was incubated at RT for 15 min prior to another washing step as above and the subsequent exposure to goat anti-human C3 (HRP-conjugate from MP Biomedicals, LLC) at a 1:1000 dilution in 1% BSA/PBS, 50 μl/well for 30 min at RT. After washing three times with PBST detection was achieved by adding 50 μl/well of a freshly mixed solution containing 0.1 M sodium citrate at pH 4.3, 5 mg ABTS (Roche) and 0.03 % H_2O_2. Absorbance was read at 405 nm. EDTA at a final concentration of 10 mM was used as negative control.

The inhibitory potency towards AP activation was evaluated by an ELISA, in which 96-well plates were coated with 40 μg/ml lipopolysaccharide (LPS) from *Salmonella typhimurium* (Sigma) in PBS pH 7.4, 50 μl/well for 2 h at RT or overnight at 4 °C. Washing, blocking, addition of analytes was performed as above. To 30 μl of analyte in PBS, 30 μl of a solution containing 50% serum and 10 mM MgEGTA in PBS was added. The mix was incubated for 1 h at 37 °C. Negative control, washing and detection were performed as described above.

PNH hemolysis assays

Inhibition of erythrocyte lysis by mini-FH, FH and its fragments was assessed by both an *in vitro* model of PNH and in cells from PNH patients. For the *in vitro* model, erythrocytes from a healthy donor were treated as described before (33), with few modifications, in order to induce PNH-like phenotype (sensitized erythrocytes). In brief, erythrocytes were treated with an 8% solution of the sulfhydryl reagent 2-aminoethylisothiouronium-bromide and then washed with PBSE (PBS pH 7.4 containing 5 mM EDTA) and PBS. The concentration of erythrocytes in PBS was adjusted so that the absorbance at 405 nm of 100 μl of a dilution of 10 μl erythrocyte stock in 190 μl water yielded a value between 1.5 and 2.0. To such a stock an anti-CD55 antibody (clone BRIC216, AbDSerotec) was added to a final concentration of 6.7 μg/ml and the mix was incubated for 30 min on ice. After washing with PBS the treated erythrocytes were resuspended with PBS-Mg (PBS containing 1 mM $MgCl_2$ at pH 6.4) to the initial volume (to yield the same concentration of erythrocytes) and subjected to the protection/lysis assay. For assays involving desialylated erythrocytes, the suspension in PBS-Mg was split in half. Both halves were incubated at 37 °C on a rotating disk, but only one had been substituted with 36 U of neuraminidase (New England Biolabs) per 100 μl of

NIH-PA Author Manuscript

NIH-PA Author Manuscript

NIH-PA Author Manuscript

erythrocyte stock. Fresh human serum was acidified with 0.2 M HCl to pH 6.4 and substituted with $MgCl_2$ and EGTA to yield final concentrations of 2.5 mM and 8 mM, respectively (similarly to (33)). In a round bottom 96 well plate, 60 μl of this serum-mix were added to 10 μl PBS at pH 6.4 containing 1 mM $MgCl_2$ and 20 μl of each inhibitor or control protein in PBS. The plate was shaken and incubated on ice for 5 min prior to pipetting 10 μl of sensitized, or sensitized and desialylated erythrocytes, into each well. The final serum concentration in this reaction mix was 52%. The 96-well plate was incubated on a shaking platform for 30 min at 37 °C and thereafter the reaction was immediately quenched by addition of 100 μl ice-cold PBS containing 5 mM EDTA. Remaining, *i.e.* non-lysed, cells were spun out at 1000 g for 3 min and 100 μl of the supernatant was transferred into a fresh 96-well plate to measure the absorbance at 405 nm. As controls, PBS or an EDTA solution (20 mM) were added instead of the protein analytes. For the determination of the reference point of total lysis, 10 μl of sensitized erythrocytes were mixed with 90 μl water. Otherwise controls were treated as the samples specified above.

Selected inhibitors were also evaluated for their protective effect against lysis of erythrocytes from PNH patients. For this purpose, blood was collected from patients (for PNH erythrocytes; EDTA tubes) or healthy individuals (for ABO-matched serum; serum tubes) after informed consent. Two patients with pure hemolytic PNH without evidence of bone marrow failure (nor any history of thromboembolic complications) and no previous transfusion were selected. Both patients showed large PNH populations in all blood lineages: patient #1 had ~30% PNH erythrocytes ($CD59^-$; ~15% of which type III) and ~90% PNH granulocytes and monocytes; patient #2 had ~15% PNH erythrocytes (almost all type III) as well as ~70% PNH granulocytes and monocytes. A 50% erythrocyte suspension (containing ~5×10^6 cells/μl) was prepared after centrifugation and 3 wash cycles in saline. Fresh sera were obtained after centrifugation of blood samples for 15 min at 1350 g and were used within 1 hour or stored at −80 °C. Serum pools from at least two healthy subjects were used to compensate for differences in complement activity between individuals; sera were obtained from three healthy subjects who had C3 and C4 blood level in the normal range by routine testing. PNH erythrocytes were incubated at final hematocrits of 2% with pooled ABO-matched sera that were supplemented with 1.5 mM $MgCl_2$. HCl was added (1:20 of 0.1 N HCl) to lower the pH (to a value of 6.7 – 6.9) and trigger activation of the AP. A concentration series (0.001-1.0 μM) of each analyte (FH, FH1-4, FH12-13, FH19-20, mini-FH) was added to the sample tubes prior to AP activation, and the samples were incubated for 24 h at 37 °C. Hemolysis was assessed after 24 hours by comparing baseline and post-incubation percentages of PNH erythrocytes using flow cytometry as described before (34, 35). C3 fragment deposition was assessed by flow cytometry using an anti-C3 polyclonal antibody (Ab14396 Abcam Inc., Cambridge, UK), as previously described (8).

Results

Design and expression of mini-FH

We designed mini-FH as a complement-targeted therapeutic by considering three main criteria. (i) To gain AP-specific efficacy, the new inhibitor should include key functional areas of FH, *i.e.,* CCP1-4 that mediates C3b binding and exerts regulatory activities, along with CCP19-20 that enhances binding to C3b and allows recognition of self-surfaces and, potentially, sites of ongoing complement activation. (ii) The protective function of FH on sites of oxidative insult should be incorporated through the CCP19-20 modules, since it was shown that the C-terminus of FH strongly binds to markers of oxidative damage (15). (iii) The two functional segments, CCP1-4 and CCP19-20, should be tethered together in such a way as to promote high-affinity binding to C3b while also allowing binding to downstream C3b-degradation products iC3b and C3dg, thereby ensuring targeting to sites of continuous complement activation and regulation (23).

NIH-PA Author Manuscript

NIH-PA Author Manuscript

NIH-PA Author Manuscript

The recently described co-crystal structures of C3b:FH1-4 (24) and C3d:FH19-20 (14) were used as starting points for the rational engineering. When these two structures were superimposed via alignment of the common TED domain in C3b and C3d (Fig. 1B), the resulting model of the tertiary complex revealed close proximity of the two FH fragments. The distance (C_α–C_α) between the alanine at the C-terminus of the FH1-4 construct and the N-terminal glycine of CCP19 (FH residue G1107; sequence numbering includes the signal peptide of FH) was 35.3 Å. To design a flexible linker with low immunogenic and aggregation potential (36), we opted for an all-glycine sequence. Given the maximum distance of 3.8 Å between two C_α-atoms of two consecutive amino acid residues, a minimum of nine glycines was needed to span 35.3 Å. Computational modeling was employed to optimize the number of linking glycines so as to provide sufficient flexibility to allow covalently tethered CCP1-4 and CCP19-20 to bind simultaneously to the same C3b molecule. *In silico* constructions of such fusion proteins in complex with C3b were subjected to scoring based on energy calculations and plotted against the number of glycine residues (Fig. 1C). The analysis revealed a two-stage relationship, in which the increase from 9-12 glycines resulted in a fast drop of energy consistent with the relaxation of local strain, whereas further elongation (13-18 glycines) retained a relaxed state with little further improvement of the energy score (Fig. 1C, Supplementary Fig. S1). A minimum of 12 glycines was therefore found to be sufficient to connect the two functional segments of FH (Fig. 1D) without imposing constraints upon simultaneous binding to C3b; thus a molecule in which CCP1-4 is tethered by 12 glycine residues to CCP19-20 was selected for recombinant production and further studies.

Mini-FH was expressed in *Pichia pastoris* in a fermenter and the recombinant protein was purified using established chromatography methods (31). Denaturing SDS-PAGE analysis of the purified protein, under both reducing and non-reducing conditions, showed a pure preparation consistent with a 43.3-kDa protein that contains multiple disulfide bridges (Fig. 1E). Electrospray ionization mass spectrometry returned a mass of 43,332.5 Da, which is in good agreement with the theoretical mass of 43,333.7 Da. The deconvoluted mass spectrum (Fig. 1F) substantiates the high level of purity.

Targeting of mini-FH to surface markers of self, damage and disease

To efficiently regulate complement activation, mini-FH needs to maintain the binding affinity of FH towards C3b but ideally regain selectivity for iC3b and C3dg to allow for effective targeting to sites of ongoing complement amplification (as likely found on diseased host cells). Using surface plasmon resonance (SPR), we therefore analyzed the binding profiles of mini-FH, FH and its key functional fragments, recombinant FH1-4 and FH19-20, towards C3b, iC3b and C3dg that was deposited on a sensor chip by a procedure that closely reflects physiological opsonization (Fig. 2). As expected, binding of FH1-4 to iC3b and C3dg was negligible when compared to C3b. Whereas FH19-20 showed similar recognition of all three opsonins, FH showed a substantial loss of binding capacity for iC3b and, especially, C3dg. In contrast, mini-FH recognized both iC3b and C3dg with substantially higher activity when compared to FH (Fig. 2A). Although the natural complexity of the convertase-deposited and FI-converted opsonin patches on the sensor chip likely contributed to the small level of heterogeneity observed in the binding plots, a reliable determination of affinity estimates could be achieved. Analysis of the binding affinities of all analytes for the main inhibitory target C3b indeed resulted in similar apparent K_D values for FH, FH1-4 and FH19-20 as determined previously (13, 24) (Fig. 2B). Importantly, mini-FH closely matched the affinity of FH for C3b (K_D ~ 1 μM), thereby exceeding the binding strength of the individual fragments.

As the C-terminus of FH is critical for distinguishing between self, foreign and altered cells on the basis of polyanionic markers, we tested whether these features are conserved in mini-

NIH-PA Author Manuscript

NIH-PA Author Manuscript

NIH-PA Author Manuscript

FH. The same panel of FH and FH-derived proteins was therefore subjected to affinity chromatography on a heparin column as a model for polyanionic host surface markers. Consistent with previous findings (13), FH1-4 was not retained on the heparin resin. FH bound to the column but was eluted before FH19-20 that showed the highest retention; mini-FH featured weaker heparin binding than FH19-20 but surpassed the activity of FH (Fig. 3A). Finally, we evaluated the selectivity of mini-FH towards sites of oxidative stress in a recently established model that showed protective effects of FH (15). In this model, mini-FH showed a similar selectivity profile for malondialdehyde-acetaldehyde (MAA)-modified BSA to FH and FH19-20. On the other hand, FH1-4, as expected, did not bind to MAA-BSA (Fig. 3B). In summary, these data demonstrate a beneficial surface-targeting profile for mini-FH, which matches or even surpasses that of FH in aspects that may be critical for therapeutic modulation of inflammatory responses.

Inhibition of complement activation

The presence of the regulatory CCP1-4 domains and the preserved affinity for C3b are expected to render mini-FH an efficient inhibitor of AP activation. Indeed, when evaluated in an established AP-specific complement activation ELISA, mini-FH showed highly potent inhibition with an IC_{50} of 0.04 μM that exceeded the activity of FH more than tenfold (IC_{50} = 0.53 μM). In comparison, FH1-4 inhibited the AP at an IC_{50} of 1.2 μM whereas FH19-20 showed no inhibitory activity (Fig. 4A). As expected, neither mini-FH nor FH and its fragments showed considerable inhibitory activity towards the classical pathway of complement activation (CP) as determined by ELISA (Fig. 4B). The selectivity of the assay system was validated by an analog of the C3-specific peptidic inhibitor compstatin (Cp30) (37), which inhibited both the AP and CP in contrast to an inactive Cp30 control peptide (Fig. 4A, 4B).

Next we evaluated whether both decay acceleration (DAA) and cofactor activities (CA) contribute to the inhibitory effect of mini-FH. For testing DAA potency, we established an AP C3 convertase complex (C3bBb) on a SPR sensor chip and monitored the decay rate in the presence and absence of FH-derived analytes. As expected, FH19-20 did not exert any activity (24, 31), whereas all analytes containing CCP1-4 potently destabilized the convertase. While the activities of FH1-4 and FH were almost identical, mini-FH showed a more pronounced DAA effect (Fig. 4C). FH and mini-FH were also probed for their ability to act as a cofactor for FI-mediated proteolytic inactivation of C3b into iC3b in solution. Both analytes exhibit cofactor-activity with FH facilitating faster consecutive cleavage of the first two scissile bonds in the α-chain of C3b (between residues 1303-1304 and 1320-1321) (38) when compared to mini-FH (Fig. 4D).

Protection of erythrocyte lysis in PNH

The therapeutic potential of mini-FH in AP-mediated disorders that involve insufficiently protected host cell surfaces was evaluated in two established models of PNH (33, 35). Analyte screening was performed in an *in vitro* model, in which a PNH-like phenotype was induced in healthy erythrocytes by impairing membrane-bound regulators prior to exposition to acidified serum, which renders them susceptible to complement-mediated lysis (33). Addition of a control fragment from the non-regulatory region of FH (*i.e.*, FH12-13) produced the same levels of lysis as PBS alone (Fig. 5A). In contrast, increasing concentrations of FH19-20 gradually increased lysis of erythrocytes due to competition with FH present in serum (the plasma concentration of FH is approximately 3.2 μM (34), which leads to a baseline level of ~1.6 μM FH at the serum dilution used throughout the assay). Addition of FH, FH1-4 and mini-FH resulted in dose-dependent protection of PNH-induced erythrocytes (Fig. 5A). Importantly, much lower concentrations were needed to reach 50% inhibition of lysis in the case of mini-FH (0.02 μM) when compared to FH (0.20 μM) or

NIH-PA Author Manuscript

NIH-PA Author Manuscript

NIH-PA Author Manuscript

FH1-4 (0.35 μM), thereby supporting a potent effect of mini-FH on surface-targeted complement activation. To further analyze the contribution of polyanionic surface markers in this activity, negatively charged sialic acid moieties, which are abundant on erythrocyte surfaces, were removed enzymatically with neuraminidase. When subjected to the same PNH assay, the ability of FH19-20 to increase lysis of PNH-induced erythrocytes was completely abolished after neuraminidase treatment. The lack of sialic acid had no effect on FH1-4, thereby confirming that neuraminidase treatment itself did not significantly alter the baseline susceptibility to lysis and establishing FH1-4 as a suitable control for the comparison of the other regulators. Conversely, both FH and mini-FH showed slightly lower inhibitory potency (Fig. 5B), which indicated partial contribution of polyanion-targeting in the overall activity of these inhibitors.

The results concerning protection of PNH erythrocytes were further validated in a previously described and disease-relevant assay using erythrocytes from PNH patients (35). After isolation, these erythrocytes were incubated in acidified ABO-matched serum in the presence of selected inhibitors or controls and monitored for hemolysis after 24 h. In absence of inhibitors, exposure to acidified serum resulted in massive (>95%) hemolysis of type III PNH erythrocytes (*i.e.*, the ones with the higher susceptibility to complement-mediated lysis both in vivo and in vitro) (39). In good agreement with the in vitro assay described above, FH and FH1-4 showed similar activity with concentrations of 1 μM or above to reach full inhibition, whereas FH19-20 and the FH12-13 control did not show any signs of inhibition. Again, mini-FH featured a much stronger activity with full inhibition around 0.1 μM and a calculated IC_{50} of 0.06 μM (Fig. 6A), thereby revealing an almost tenfold activity gain of the engineered inhibitor when compared to the parent protein. Furthermore, consistent with this mechanism of action, effective concentrations of mini-FH also prevent deposition of C3 fragments on PNH erythrocyte surfaces (Fig. 6B-E); such complement fixation had been described as an *in vitro* marker of C3-mediated extravascular hemolysis, which is a well-established phenomenon limiting the efficacy of C5-based complement inhibition (35) and has been reproduced *in vitro* after exposure to AP activation of sera containing the therapeutic C5 antibody Eculizumab (35).

Discussion

Our approach of rationally selecting and combining six out of 20 modules of FH, thereby achieving a 68% reduction in polypeptide size (and a 72% reduction in overall molecular weight due to concomitant exclusion of all eight N-glycosylation sites in FH), resulted in an AP-selective complement inhibitor with promising clinical potential. Intriguingly, such a condensation into a smaller molecule of targeted complement-regulatory activity may be compared with the complement evasion strategies that have evolved in several orthopox viruses; for example, vaccinia virus secretes a regulator mimic (VCP) that combines several functions, *i.e.,* heparin binding and regulatory activities towards both the alternative and classical pathway, in just four CCP domains (40). Whereas immunogenicity issues likely prevent a direct therapeutic application of such viral mimics, our use of host regulatory domains in mini-FH fused by a polyglycine linker (36) is expected to circumvent this concern. Mini-FH could be efficiently produced in *P. pastoris* as a homogeneous product with high yield and purity. As mini-FH does not contain any glycosylation sites (in contrast to the parent protein FH (31)), yeast is considered highly suitable for the production of the inhibitor and is likely to offer significant advantages over mammalian expression system with respect to ease-of-manufacturing, production yield and cost effectiveness.

On balance, mini-FH preserves the mode of action and versatility of the parent molecule. Despite the substitution of the 14-domain core region of FH with a short polyglycine linker, mini-FH largely retained the binding affinity for C3b, thereby indicating simultaneous

NIH-PA Author Manuscript

NIH-PA Author Manuscript

NIH-PA Author Manuscript

binding to both sites. Cofactor activity in solution was less efficient for mini-FH, especially concerning the second cleavage to iC3b. Speculatively, this difference might originate in the higher flexibility of mini-FH relative to FH that may be less efficient in stabilizing conformational states in C3b that have been thought to facilitate binding and cleavage by FI (24). The decay acceleration activity of mini-FH, on the other hand, appeared significantly increased in the SPR assay. While extended structure-function studies may shed more light into exact mechanistic differences, it is already evident that mini-FH acts on the convertase and C3b and that its overall AP-inhibitory activity surpasses that of the parent FH. However, mini-FH also introduces a novel functionality. The proposed cryptic nature of the TED-binding site in CCP 19-20 has been eliminated by engineering, so that mini-FH binds directly and much more efficiently to downstream complement opsonins than FH. Together with its observed pattern-recognition capability for polyanionic host- and oxidative damage-related surface markers, mini-FH is equipped with a unique triple-targeting mechanism that appears ideally suited for the regulation of complement activation on diseased and altered host surfaces.

This potential benefit has clearly been indicated in both models of PNH, where mini-FH featured a tenfold improvement over FH. Erythrocytes from PNH patients are susceptible to AP-mediated lysis due to the lack of two GPI-anchored complement regulators (CD55, CD59) on their surface (4, 41-44). Interestingly, the residual regulators on the erythrocyte surface (CD35) and in circulation (FH, FI) still control AP activation but appear insufficient to compensate for the loss of CD55 and CD59 (34, 45). Therapeutic blockage of MAC formation by the clinical C5 antibody Eculizumab (Soliris; Alexion) offers a costly yet effective option to control intravascular hemolysis and related symptoms in PNH, with a remarkable clinical benefit in most patients. However, Eculizumab acts downstream in the complement cascade and does not interrupt AP amplification, thereby leading to an increasing fraction of heavily C3-opsonized PNH erythrocytes that eventually become susceptible to extravascular hemolysis after recognition by immune cells (8). As a consequence, a considerable fraction of PHN patients treated with Eculizumab show residual anemia relying on an additional pathogenic mechanism, which may result in persistent transfusion-dependency regardless of blocking the formation of lytic pores (8, 9, 46-48). The need for therapeutics that act at the level of AP amplification has therefore been recognized. In fact, the targeted FH-based fusion protein (TT30, ALXN1102; Alexion), which combines FH CCP1-5 with the CCP1-4 of CR2 (see above), is currently being evaluated in a phase I clinical trial (http://www.clinicaltrials.gov/ct2/show/NCT01335165). Whereas the binding specificity of CR2 for iC3b and C3dg (but not C3b) confers a similar targeting profile towards sites of ongoing complement turnover as observed in mini-FH, TT30 is not equipped with the recognition capabilities of mini-FH for patterns of self-surfaces and oxidative stress. Notably, TT30 only contains a single binding region for C3b. Moreover, in TT30 the iC3b/C3dg targeting region is directly fused onto the N-terminus of FH1-5, which likely renders simultaneous binding to C3b and the target surface more difficult or complex with possible implications on regulatory activity The recent evaluation of TT30 in the same PNH assay as used in this study indeed indicated a lower inhibitory activity (IC_{50} ~ 0.5 μM) (35) when compared to the activity of mini-FH described here (IC_{50} ~ 0.06 μM), yet a direct comparison between different inhibitors in the same assay will be necessary for better elucidating the effects of distinct targeting strategies.

Targeted complement inhibitors such as TT30 and its homologs have not only shown promising potential in PNH but also in a variety of other AP-mediated clinical conditions ranging from collagen-induced arthritis and ischemia/reperfusion injury to AMD (23, 49). In the case of AMD, mini-FH may have particular advantages. This chronic and progressive eye disease, which leads to loss of vision due to geographic atrophy and/or neovascularization of retinal tissue, is strongly associated with impaired complement

NIH-PA Author Manuscript

NIH-PA Author Manuscript

NIH-PA Author Manuscript

regulation by FH. Furthermore, FH was recently identified as a major binding protein for the lipid peroxidation products MDA and MAA, which are markers of oxidative stress and accumulate under various disease conditions including AMD (15, 50). Disorders such as atherosclerosis or Alzheimer's disease have also been reported to show a similar association between oxidative stress and complement activation (50-52). Our assays with MAA-modified protein surfaces demonstrated that mini-FH largely preserves selective recognition of these disease markers and may therefore be targeted to such sites of oxidative stress damage. Even in the absence of oxidative markers, diseases with excessive and/or poorly regulated complement activity such as atypical hemolytic uremic syndrome or dense deposit disease could benefit greatly from simultaneous targeting to sites of ongoing inflammation and self-specific molecular markers such as GAGs or sialic acid.

Even though several systemic complement inhibitors evaluated to date displayed beneficial safety profiles in clinical trials, concern has been expressed that the long-term complement inhibition needed in chronic diseases, such as PNH, may compromise the physiological roles of complement in immune homeostasis or microbial defense. For example, patients undergoing systemic Eculizumab treatment receive vaccination against Neisserial infections as a preventive measure (53). In this respect, the targeting of C3b degradation products that predominantly appear on opsonized host cells under disease conditions, confers the advantage of introducing an additional selectivity factor for host-over foreign surfaces. In an *in vivo* model of sepsis, it was shown that targeting a mouse homolog of TT30 (*i.e.,* CR2-Crry) to sites of ongoing complement inactivation was not only significantly more effective in preventing injury but also avoided host susceptibility to infection as had been observed during non-targeted complement inhibition (10). Furthermore, surface-targeted inhibitors may be less dependent on the plasma drug concentration and half-life but rather on the local concentration on the target cell or tissue; TT30, for example, showed a long residence time on erythrocytes and AP inhibition of up to 24 h after subcutaneous injection (23). Similar concepts may apply for mini-FH, yet both local and systemic residence profiles need to be further investigated. While the current size of 43 kDa likely allows some degree of renal filtration, optimization strategies for decreasing elimination of recombinant proteins have been described (36, 54) and may be considered depending on the pharmacokinetic analysis of mini-FH.

Besides the therapeutic implications, our study also revealed important insight about FH as a surface-targeted regulator. Removal of the central modules (CCP5-18) in mini-FH did not hamper but actually increased the inhibitory potency tenfold over FH in the AP activation assay and in both models of PNH. As the C3b-binding affinity and regulatory mechanisms of mini-FH are similar to FH, it is likely that it is the surface-targeting effect of an accessible C3b/iC3b/C3dg-binding site in mini-FH that has led to increased activity. This is borne out by the poor binding of intact native human FH to iC3b and C3d, indicating that the C3b/iC3b/C3dg-binding site present within CCPs 19-20 is indeed cryptic, which is in agreement with a proportion of previous observations (20, 21). Current models suggest that FH is capable of adopting a complex and compactly folded-back conformation whereby both termini are positioned close to one another (14, 27). This is consistent with the binding site for TED/C3d being partially occluded by the steric bulk of other CCP modules in FH. It may be that this cryptic site is only revealed after binding of CCP1-4 to C3b. While this mode of action may be appropriate for regulation of the AP in solution and on healthy cells, which are usually exposed to marginal opsonization, such a strategy may be inadequate under disease conditions where C3b quickly accumulates on a surface. Under these conditions in which surface-attached iC3b and C3dg are also produced in large numbers mini-FH is more effective. It should be noted that the middle region of FH may not only have a structural role but also contains an additional polyanion-recognizing region (CCP6-8); however, this site does not seem to be needed for effective complement regulation in the models used in this

NIH-PA Author Manuscript

NIH-PA Author Manuscript

NIH-PA Author Manuscript

study and is considered less suitable for targeting strategies due to its lack of opsonin binding.

Taken together, our study underscores the great potential of exploiting the modular architecture of the RCA family of complement regulators for the rational engineering of therapeutic inhibitors. The development of mini-FH directly benefited from recent structural data of FH, yet at the same time provided valuable insight into the function of this key AP regulator. Importantly, the high inhibitory activity and unique targeting profile of mini-FH may prove highly beneficial for use in a wide spectrum of disease models that involve AP-mediated attack of host cells and tissues. Whereas aspects such as pharmacokinetic properties need to be further investigated, the promising results in models of PNH and the positive experience with RCA-based inhibitors such as TT30 or soluble CR1 suggests good prospects for clinical development of mini-FH.

Supplementary Material

Refer to Web version on PubMed Central for supplementary material.

Acknowledgments

We thank Dr. Hui Chen for his support in the mass spectrometric characterization of mini-FH.

This work was supported by National Institutes of Health grants AI030040, AI068730, AI072106, and EY020633.

Abbreviations used

AMD	age-related macular degeneration
AP	alternative pathway
C1-INH	C1 inhibitor
CCP	complement control protein domain
CP	classical pathway
FH	factor H
GAG	glycosaminoglycan
MAA	malondialdehyde-acetaldehyde
MDA	malondialdehyde
PNH	paroxysmal nocturnal hemoglobinuria
SPR	surface plasmon resonance
TED	thioester-containing domain

References

1. Ricklin D, Hajishengallis G, Yang K, Lambris JD. Complement: a key system for immune surveillance and homeostasis. Nat. Immunol. 2010; 11:785–97. [PubMed: 20720586]
2. Kohl J. The role of complement in danger sensing and transmission. Immunol. Res. 2006; 34:157–76. [PubMed: 16760575]
3. Zipfel PF, Skerka C. Complement regulators and inhibitory proteins. Nat. Rev. Immunol. 2009; 9:729–40. [PubMed: 19730437]
4. Parker CJ. The pathophysiology of paroxysmal nocturnal hemoglobinuria. Exp. Hematol. 2007; 35:523–33. [PubMed: 17379062]

NIH-PA Author Manuscript

NIH-PA Author Manuscript

NIH-PA Author Manuscript

5. Ricklin D, Lambris JD. Complement-targeted therapeutics. Nat. Biotechnol. 2007; 25:1265–75. [PubMed: 17989689]
6. Skattum L, van Deuren M, van der Poll T, Truedsson L. Complement deficiency states and associated infections. Mol. Immunol. 2011; 48:1643–55. [PubMed: 21624663]
7. Harboe M, Ulvund G, Vien L, Fung M, Mollnes TE. The quantitative role of alternative pathway amplification in classical pathway induced terminal complement activation. Clin. Exp. Immunol. 2004; 138:439–46. [PubMed: 15544620]
8. Risitano AM, Notaro R, Marando L, Serio B, Ranaldi D, Seneca E, Ricci P, Alfinito F, Camera A, Gianfaldoni G, Amendola A, Boschetti C, Di Bona E, Fratellanza G, Barbano F, Rodeghiero F, Zanella A, Iori AP, Selleri C, Luzzatto L, Rotoli B. Complement fraction 3 binding on erythrocytes as additional mechanism of disease in paroxysmal nocturnal hemoglobinuria patients treated by eculizumab. Blood. 2009; 113:4094–100. [PubMed: 19179465]
9. Risitano AM, Perna F, Selleri C. Achievements and limitations of complement inhibition by eculizumab in paroxysmal nocturnal hemoglobinuria: the role of complement component 3. Mini Rev. Med. Chem. 2011; 11:528–35. [PubMed: 21561403]
10. Atkinson C, Song H, Lu B, Qiao F, Burns TA, Holers VM, Tsokos GC, Tomlinson S. Targeted complement inhibition by C3d recognition ameliorates tissue injury without apparent increase in susceptibility to infection. J. Clin. Invest. 2005; 115:2444–53. [PubMed: 16127466]
11. Ricklin D, Lambris JD. Progress and trends in complement therapeutics. Adv. Exp. Med. Biol. 2013; 735:1–22. [PubMed: 23402016]
12. Holers VM, Rohrer B, Tomlinson S. CR2-mediated targeting of complement inhibitors: bench-to-bedside using a novel strategy for site-specific complement modulation. Adv. Exp. Med. Biol. 2013; 735:137–54. [PubMed: 23402024]
13. Schmidt CQ, Herbert AP, Kavanagh D, Gandy C, Fenton CJ, Blaum BS, Lyon M, Uhrin D, Barlow PN. A new map of glycosaminoglycan and C3b binding sites on factor H. J. Immunol. 2008; 181:2610–9. [PubMed: 18684951]
14. Morgan HP, Schmidt CQ, Guariento M, Blaum BS, Gillespie D, Herbert AP, Kavanagh D, Mertens HD, Svergun DI, Johansson CM, Uhrin D, Barlow PN, Hannan JP. Structural basis for engagement by complement factor H of C3b on a self surface. Nat. Struct. Mol. Biol. 2011; 18:463–70. [PubMed: 21317894]
15. Weismann D, Hartvigsen K, Lauer N, Bennett KL, Scholl HP, Charbel Issa P, Cano M, Brandstatter H, Tsimikas S, Skerka C, Superti-Furga G, Handa JT, Zipfel PF, Witztum JL, Binder CJ. Complement factor H binds malondialdehyde epitopes and protects from oxidative stress. Nature. 2011; 478:76–81. [PubMed: 21979047]
16. Aslam M, Perkins SJ. Folded-back solution structure of monomeric factor H of human complement by synchrotron X-ray and neutron scattering, analytical ultracentrifugation and constrained molecular modelling. J. Mol. Biol. 2001; 309:1117–38. [PubMed: 11399083]
17. Meri S, Pangburn MK. Discrimination between activators and nonactivators of the alternative pathway of complement: regulation via a sialic acid/polyanion binding site on factor H. Proc. Natl. Acad. Sci. U.S.A. 1990; 87:3982–6. [PubMed: 1692629]
18. Schmidt CQ, Herbert AP, Hocking HG, Uhrin D, Barlow PN. Translational mini-review series on complement factor H: structural and functional correlations for factor H. Clin. Exp. Immunol. 2008; 151:14–24. [PubMed: 18081691]
19. Ferreira VP, Herbert AP, Hocking HG, Barlow PN, Pangburn MK. Critical role of the C-terminal domains of factor H in regulating complement activation at cell surfaces. J. Immunol. 2006; 177:6308–16. [PubMed: 17056561]
20. Ross GD, Newman SL, Lambris JD, Devery-Pocius JE, Cain JA, Lachmann PJ. Generation of three different fragments of bound C3 with purified factor I or serum. II. Location of binding sites in the C3 fragments for factors B and H, complement receptors, and bovine conglutinin. J. Exp. Med. 1983; 158:334–52. [PubMed: 6224880]
21. Alcorlo M, Martinez-Barricarte R, Fernandez FJ, Rodriguez-Gallego C, Round A, Vega MC, Harris CL, de Cordoba SR, Llorca O. Unique structure of iC3b resolved at a resolution of 24 A by 3D-electron microscopy. Proc. Natl. Acad. Sci. U.S.A. 2011; 108:13236–40. [PubMed: 21788512]

NIH-PA Author Manuscript

NIH-PA Author Manuscript

NIH-PA Author Manuscript

22. Oppermann M, Manuelian T, Jozsi M, Brandt E, Jokiranta TS, Heinen S, Meri S, Skerka C, Gotze O, Zipfel PF. The C-terminus of complement regulator Factor H mediates target recognition: evidence for a compact conformation of the native protein. Clin. Exp. Immunol. 2006; 144:342–52. [PubMed: 16634809]

23. Fridkis-Hareli M, Storek M, Mazsaroff I, Risitano AM, Lundberg AS, Horvath CJ, Holers VM. Design and development of TT30, a novel C3d-targeted C3/C5 convertase inhibitor for treatment of human complement alternative pathway-mediated diseases. Blood. 2011; 118:4705–13. [PubMed: 21860027]

24. Wu J, Wu YQ, Ricklin D, Janssen BJ, Lambris JD, Gros P. Structure of complement fragment C3b-factor H and implications for host protection by complement regulators. Nat. Immunol. 2009; 10:728–33. [PubMed: 19503104]

25. Kajander T, Lehtinen MJ, Hyvarinen S, Bhattacharjee A, Leung E, Isenman DE, Meri S, Goldman A, Jokiranta TS. Dual interaction of factor H with C3d and glycosaminoglycans in host-nonhost discrimination by complement. Proc. Natl. Acad. Sci. U.S.A. 2011; 108:2897–902. [PubMed: 21285368]

26. Sali A, Blundell TL. Comparative protein modelling by satisfaction of spatial restraints. J. Mol. Biol. 1993; 234:779–815. [PubMed: 8254673]

27. Schmidt CQ, Herbert AP, Mertens HD, Guariento M, Soares DC, Uhrin D, Rowe AJ, Svergun DI, Barlow PN. The central portion of factor H (modules 10-15) is compact and contains a structurally deviant CCP module. J. Mol. Biol. 2010; 395:105–22. [PubMed: 19835885]

28. Jokiranta TS, Westin J, Nilsson UR, Nilsson B, Hellwage J, Lofas S, Gordon DL, Ekdahl KN, Meri S. Complement C3b interactions studied with surface plasmon resonance technique. Int. Immunopharmacol. 2001; 1:495–506. [PubMed: 11367533]

29. Harris CL, Abbott RJ, Smith RA, Morgan BP, Lea SM. Molecular dissection of interactions between components of the alternative pathway of complement and decay accelerating factor (CD55). J. Biol. Chem. 2005; 280:2569–78. [PubMed: 15536079]

30. Nilsson UR, Funke L, Nilsson B, Ekdahl KN. Two conformational forms of target-bound iC3b that distinctively bind complement receptors 1 and 2 and two specific monoclonal antibodies. Ups. J. Med. Sci. 2011; 116:26–33. [PubMed: 21070093]

31. Schmidt CQ, Slingsby FC, Richards A, Barlow PN. Production of biologically active complement factor H in therapeutically useful quantities. Protein. Expr. Purif. 2011; 76:254–63. [PubMed: 21146613]

32. Leemans JC, Cassel SL, Sutterwala FS. Sensing damage by the NLRP3 inflammasome. Immunol. Rev. 2011; 243:152–62. [PubMed: 21884174]

33. Ezzell JL, Wilcox LA, Bernshaw NJ, Parker CJ. Induction of the paroxysmal nocturnal hemoglobinuria phenotype in normal human erythrocytes: effects of 2-aminoethylisothiouronium bromide on membrane proteins that regulate complement. Blood. 1991; 77:2764–73. [PubMed: 1710519]

34. Ferreira VP, Pangburn MK. Factor H mediated cell surface protection from complement is critical for the survival of PNH erythrocytes. Blood. 2007; 110:2190–2. [PubMed: 17554058]

35. Risitano AM, Notaro R, Pascariello C, Sica M, Del Vecchio L, Horvath CJ, Fridkis-Hareli M, Selleri C, Lindorfer MA, Taylor RP, Luzzatto L, Holers VM. The complement receptor 2/factor H fusion protein TT30 protects paroxysmal nocturnal hemoglobinuria erythrocytes from complement-mediated hemolysis and C3 fragment. Blood. 2012; 119:6307–16. [PubMed: 22577173]

36. Schellenberger V, Wang CW, Geething NC, Spink BJ, Campbell A, To W, Scholle MD, Yin Y, Yao Y, Bogin O, Cleland JL, Silverman J, Stemmer WP. A recombinant polypeptide extends the in vivo half-life of peptides and proteins in a tunable manner. Nat. Biotechnol. 2009; 27:1186–90. [PubMed: 19915550]

37. Qu H, Ricklin D, Bai H, Chen H, Reis ES, Maciejewski M, Tzekou A, Deangelis RA, Resuello RR, Lupu F, Barlow PN, Lambris JD. New analogs of the clinical complement inhibitor compstatin with subnanomolar affinity and enhanced pharmacokinetic properties. Immunobiology. 2013; 218:496–505. [PubMed: 22795972]

NIH-PA Author Manuscript

NIH-PA Author Manuscript

NIH-PA Author Manuscript

38. Sahu A, Isaacs SN, Soulika AM, Lambris JD. Interaction of vaccinia virus complement control protein with human complement proteins: factor I-mediated degradation of C3b to iC3b1 inactivates the alternative complement pathway. J. Immunol. 1998; 160:5596–604. [PubMed: 9605165]
39. Rosse WF, Dacie JV. Immune lysis of normal human and paroxysmal nocturnal hemoglobinuria (PNH) red blood cells. I. The sensitivity of PNH red cells to lysis by complement and specific antibody. J. Clin. Invest. 1966; 45:736–48.
40. Smith SA, Mullin NP, Parkinson J, Shchelkunov SN, Totmenin AV, Loparev VN, Srisatjaluk R, Reynolds DN, Keeling KL, Justus DE, Barlow PN, Kotwal GJ. Conserved surface-exposed K/R-X-K/R motifs and net positive charge on poxvirus complement control proteins serve as putative heparin binding sites and contribute to inhibition of molecular interactions with human endothelial cells: a novel mechanism for evasion of host defense. J. Virol. 2000; 74:5659–66. [PubMed: 10823874]
41. Nicholson-Weller A, March JP, Rosenfeld SI, Austen KF. Affected erythrocytes of patients with paroxysmal nocturnal hemoglobinuria are deficient in the complement regulatory protein, decay accelerating factor. Proc. Natl. Acad. Sci. U.S.A. 1983; 80:5066–70. [PubMed: 6576376]
42. Pangburn MK, Schreiber RD, Muller-Eberhard HJ. Deficiency of an erythrocyte membrane protein with complement regulatory activity in paroxysmal nocturnal hemoglobinuria. Proc. Natl. Acad. Sci. U.S.A. 1983; 80:5430–4. [PubMed: 6225118]
43. Medof ME, Kinoshita T, Silber R, Nussenzweig V. Amelioration of lytic abnormalities of paroxysmal nocturnal hemoglobinuria with decay-accelerating factor. Proc. Natl. Acad. Sci. U.S.A. 1985; 82:2980–4. [PubMed: 2581259]
44. Holguin MH, Fredrick LR, Bernshaw NJ, Wilcox LA, Parker CJ. Isolation and characterization of a membrane protein from normal human erythrocytes that inhibits reactive lysis of the erythrocytes of paroxysmal nocturnal hemoglobinuria. J. Clin. Invest. 1989; 84:7–17. [PubMed: 2738160]
45. Roberts WN, Wilson JG, Wong W, Jenkins DE Jr. Fearon DT, Austen KF, Nicholson-Weller A. Normal function of CR1 on affected erythrocytes of patients with paroxysmal nocturnal hemoglobinuria. J. Immunol. 1985; 134:512–7. [PubMed: 2578050]
46. Schrezenmeier H, Hochsmann B. Drugs that inhibit complement. Transfus. Apher. Sci. 2012; 46:87–92. [PubMed: 22169380]
47. Luzzatto L, Risitano AM, Notaro R. Paroxysmal nocturnal hemoglobinuria and eculizumab. Haematologica. 2010; 95:523–6. [PubMed: 20378572]
48. Risitano AM, Notaro R, Luzzatto L, Hill A, Kelly R, Hillmen P. Paroxysmal nocturnal hemoglobinuria--hemolysis before and after eculizumab. N. Engl. J. Med. 2010; 363:2270–2. [PubMed: 21121856]
49. Rohrer B, Coughlin B, Bandyopadhyay M, Holers VM. Systemic Human CR2-Targeted Complement Alternative Pathway Inhibitor Ameliorates Mouse Laser-Induced Choroidal Neovascularization. J. Ocul. Pharmacol. Ther. 2012; 28:402–9. [PubMed: 22309197]
50. Weismann D, Binder CJ. The innate immune response to products of phospholipid peroxidation. Biochim. Biophys. Acta. 2012; 1818:2465–75. [PubMed: 22305963]
51. Machalinska A, Kawa MP, Marlicz W, Machalinski B. Complement system activation and endothelial dysfunction in patients with age-related macular degeneration (AMD): possible relationship between AMD and atherosclerosis. Acta Ophthalmol. 2011; 90:695–703. [PubMed: 22067048]
52. Ohno-Matsui K. Parallel findings in age-related macular degeneration and Alzheimer's disease. Prog. Retin. Eye Res. 2011; 30:217–38. [PubMed: 21440663]
53. Dmytrijuk A, Robie-Suh K, Cohen MH, Rieves D, Weiss K, Pazdur R. FDA report: eculizumab (Soliris) for the treatment of patients with paroxysmal nocturnal hemoglobinuria. Oncologist. 2008; 13:993–1000. [PubMed: 18784156]
54. Schlapschy M, Theobald I, Mack H, Schottelius M, Wester HJ, Skerra A. Fusion of a recombinant antibody fragment with a homo-amino-acid polymer: effects on biophysical properties and prolonged plasma half-life. Protein Eng. Des. Sel. 2007; 20:273–84. [PubMed: 17595342]

NIH-PA Author Manuscript
NIH-PA Author Manuscript
NIH-PA Author Manuscript

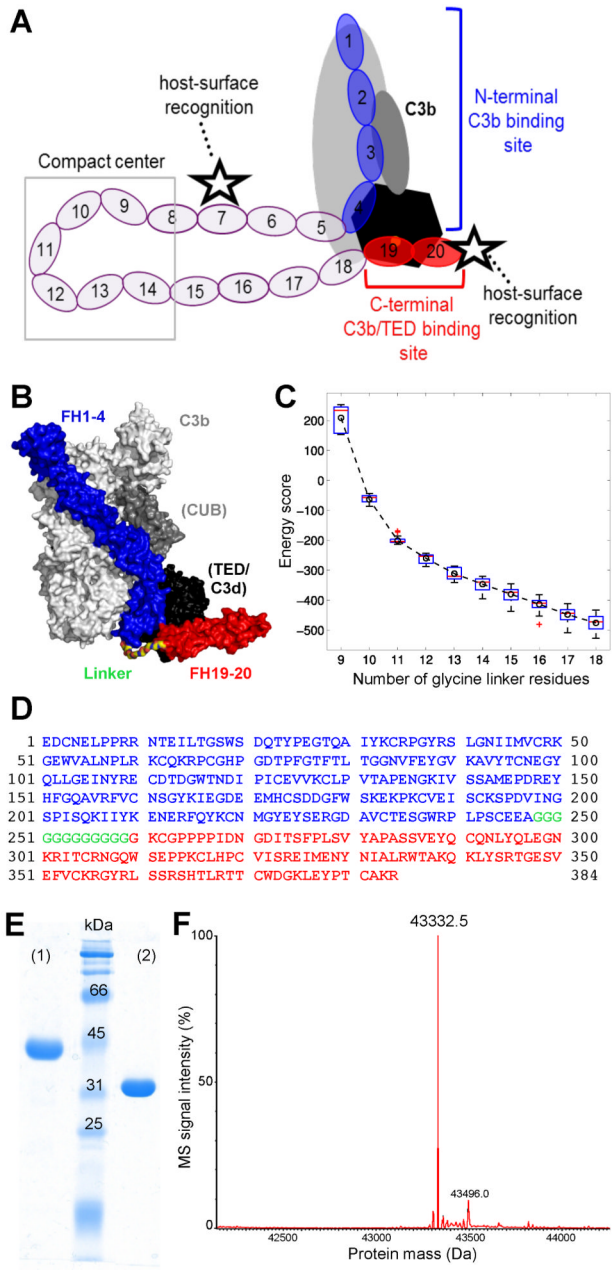

FIGURE 1.

Design and characterization of mini-FH. **(A)** Schematic representation of FH binding to complement opsonins (mainly C3b) and host surface markers. Whereas CCP domains 1-4 (blue) bind to C3b (grey/black) and exert regulatory activities, CCP19-20 (red) recognize polyanionic surface patches (star symbol) and binds to the TED domain (black) of C3b, iC3b and C3dg. **(B)** Superimposition of the co-crystal structures of C3b:FH1-4 (PDB 2WII) (24) and C3d:FH19-20 (PDB 3OXU) (14). A polyglycine linker (colored by element) combining the C-terminus of FH1-4 (blue) with the N-terminus of FH19-20 (red) was designed by molecular modeling. All residues are shown as surface representation. C3b is shown in light grey with the CUB and TED domains highlighted dark grey and black, respectively. C3d, which corresponds to TED, is also shown in black. **(C)** Energy score of modeled complexes versus number of glycine residues in the linker. The box plot shows the

NIH-PA Author Manuscript

NIH-PA Author Manuscript

NIH-PA Author Manuscript

energy score distribution based on the top 80 models of each linker length. The circle and dashed line show the change of the average energy of these linkers. A linker length of 12 glycines was selected for this study. **(D)** Amino acid sequence of mini-FH with residues derived from FH1-4 construct and FH CCP19-20 marked in blue and red, respectively. The 12 residue long polyglycine linker is marked in green. Please note that the FH1-4 construct used in this study, and previously in the crystal structure of C3b:FH1-4 (24), contains an additional alanine residue following the native C-terminus (E264) of FH CCP4. Due to the alpha-mating secretion signal of the Pichia-expression vector and the restriction enzyme used for cloning, the secretion and cloning artifact EAEAAG precedes the FH-derived residues at the N-terminus accounting for the total theoretical mass of 43,333.7 Da. **(E)** Characterization of mini-FH by SDS-PAGE (12% gel, Coomassie staining). Mini-FH emerges as a single clean band at the expected size under both reducing (1) and non-reducing (2) conditions; faster mobility in (2) indicates presence of disulfide bonds. **(F)** Mass-spectrometric analysis of mini-FH. The deconvoluted mass spectrum shows one dominant peak at 43,332.5 Da, which is consistent with the theoretical mass mini-FH and attests identity and high purity of the preparation.

NIH-PA Author Manuscript
NIH-PA Author Manuscript
NIH-PA Author Manuscript

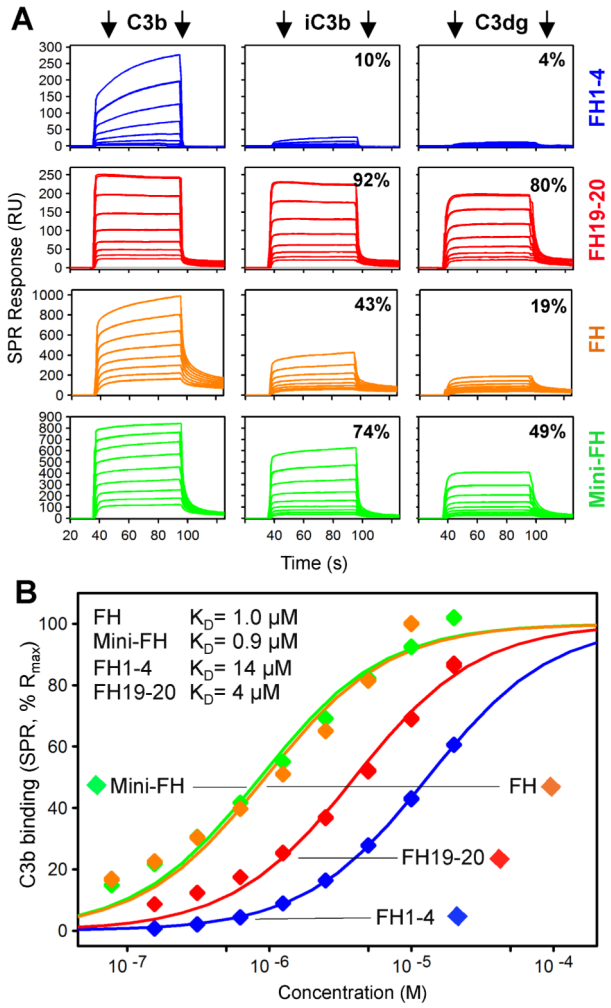

FIGURE 2.

Binding activity and specificity of mini-FH and FH-derived proteins to C3 opsonins. **(A)** Relative binding of FH, mini-FH, FH1-4 and FH19-20 to deposited opsonins C3b, iC3b and C3dg as determined by SPR. Responses were normalized to the highest signal within each set of analyte. **(B)** SPR-derived apparent binding affinities of all four analytes for C3b. Steady state responses were fitted to a single-site model and normalized for binding capacity.

NIH-PA Author Manuscript

NIH-PA Author Manuscript

NIH-PA Author Manuscript

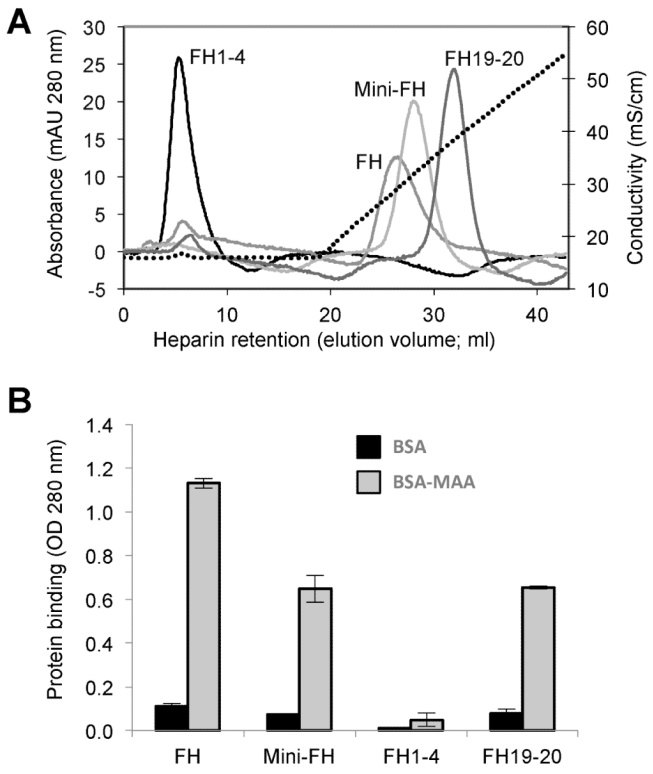

FIGURE 3.

Binding activity of mini-FH and FH-derived proteins to markers of self cells and oxidative stress. **(A)** Glycosaminoglycan binding as determined by heparin chromatography. Retention time during a NaCl gradient (0.15-0.5 M in phosphate buffer pH 7.4) signifies adhesion to heparin as model of polyanionic host surface pattern. **(B)** Recognition of oxidative damage markers. Binding of FH-derived proteins to surfaces coated with BSA or BSA modified with the lipid peroxidation product malondialdehyde-acetaldehyde (MAA-BSA) were analyzed by ELISA (detection with a polyclonal anti-FH Ab).

NIH-PA Author Manuscript
NIH-PA Author Manuscript
NIH-PA Author Manuscript

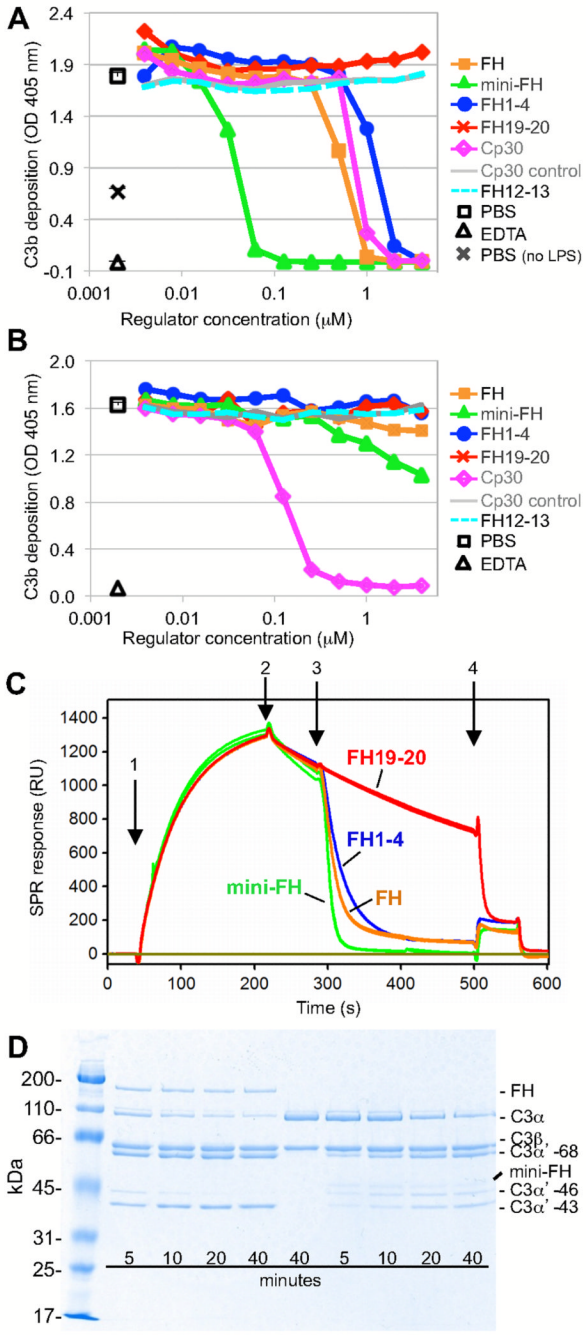

FIGURE 4.

Functional characterization of mini-FH. **(A)** Inhibition of AP activation. The inhibitory potency of mini-FH and FH-derived proteins in normal human serum was determined by ELISA after specific stimulation of AP activation with lipopolysaccharide and measurement of C3b/iC3b deposition. Compstatin analog Cp30 and an inactive Cp30 control peptide were included as positive and negative controls, respectively. Each ELISA is a representative of three independently performed assays. **(B)** Inhibition of CP activation. An antibody/antigen complex was used to specifically trigger the CP in this ELISA; detection and controls were performed in analogy to the AP-specific ELISA. **(C)** Assessment of decay acceleration activity by SPR. After on-chip formation of the AP C3 convertase (C3BbB) by injecting FB

and FD onto immobilized C3b (1) and monitoring of regular convertase decay (2), FH-derived analytes were injected at 100 nM (3) to evaluate acceleration of the decay rate; finally FH1-4 was injected at 2 μM (4) to remove residual Bb. **(D)** Evaluation of cofactor activity. C3b, FI and either FH or mini-FH were incubated in solution and the generation of iC3b was monitored over time using SDS-PAGE. Disappearance of the α' chain (114 kDa) with appearance of three new bands at 68 kDa, 46 kDa ($iC3b_1$) and 43 kDa ($iC3b_2$) indicates degradation of C3b.

NIH-PA Author Manuscript
NIH-PA Author Manuscript
NIH-PA Author Manuscript

NIH-PA Author Manuscript
NIH-PA Author Manuscript
NIH-PA Author Manuscript

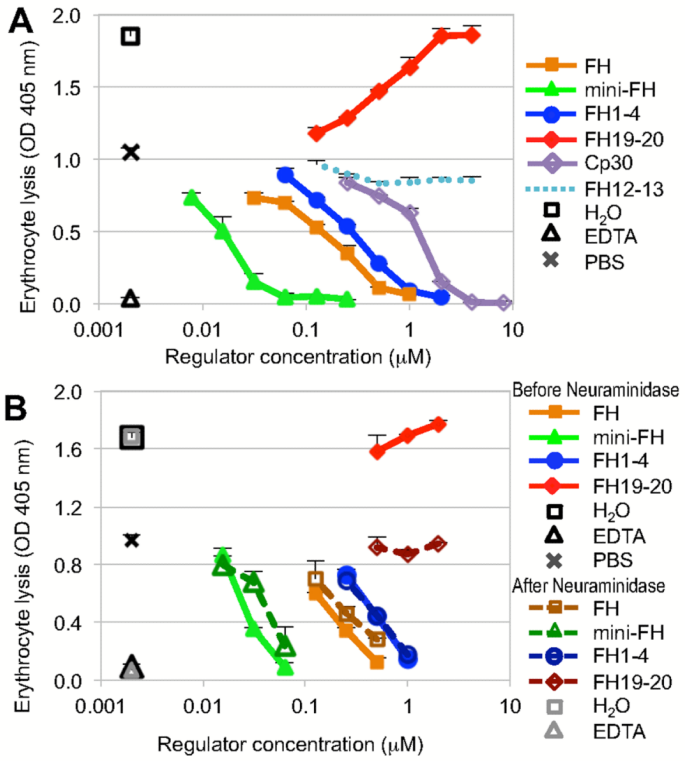

FIGURE 5.

Protection of erythrocytes with PNH-induced phenotype from AP-mediated lysis. **(A)** In an in vitro model of PNH, acidified serum was spiked with analytes prior to co-incubation with sensitized erythrocytes. Lysis was determined by measuring absorbance at 405 nm. EDTA and PBS were used as positive and negative inhibition controls, respectively; Absorbance of erythrocytes suspended in water was used to determine maximum lysis. Plot shows a representative of three independent assays. Analytes measured at a single concentration point were analyzed as triplicates, all others in duplicates; standard deviation is shown. **(B)** In order to determine the influence of polyanion-targeting on inhibitory potency, the PNH assay described above was repeated with erythrocytes before and after treatment with neuraminidase to remove sialic acid from the surface. As in panel *A*, EDTA was used as a positive inhibitory control and absorbance of total lysis was determined in water. The pair of overlapping FH1-4 curves (FH1-4 does not contain any polyanionic host-surface recognition patch) serves as a reference for all other analytes. Plot shows a representative of two independent assays.

NIH-PA Author Manuscript
NIH-PA Author Manuscript
NIH-PA Author Manuscript

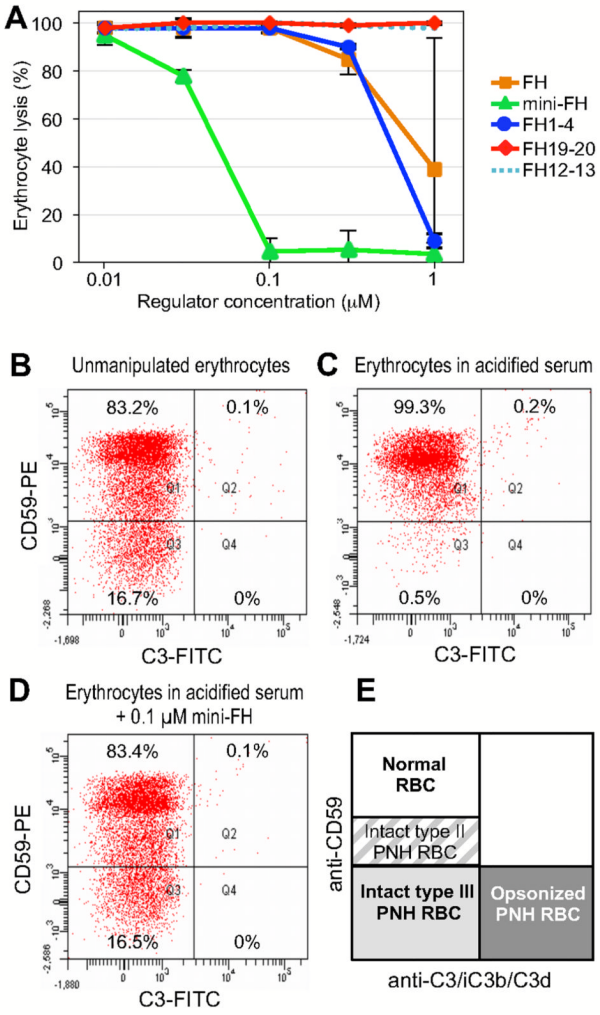

FIGURE 6.

Protection of PNH erythrocytes from AP-mediated lysis. **(A)** Erythrocytes were isolated from patient's blood and incubated in acidified serum from ABO-matched healthy donors in the presence of various analytes, and lysis was determined after 24 h. **(B-D)** Prevention of C3 fragment deposition on PNH erythrocytes. Erythrocytes from patient's blood (PNH patient #1) were exposed to AP activation by incubation in ABO-matched acidified serum. C3 deposition on PNH erythrocytes was assessed using an anti-C3 polyclonal antibody in combination with a counter staining with an anti-CD59 monoclonal antibody (35). Exposure to AP activation led to total disappearance of type III PNH erythrocytes (C) in comparison to freshly isolated erythrocytes (B). Mini-FH resulted in a full protection from lysis of type III PNH erythrocytes, without detectable deposition of C3 fragments on their surface (D). The scheme in panel E illustrates classification of erythrocytes as a function of surface molecules present (type II and type III PNH erythrocytes are defined according to the expression of CD59).